RESEARCH PAPER

Neurogenesis 2:1, e1057313; January–December 2015; Published with license by Taylor and Francis Group, LLC

Dissecting the role of Wnt signaling and its interactions with FGF signaling during midbrain neurogenesis

Carlene Dyer[1], Eric Blanc[2], Rob J Stanley[3,4], and Robert D Knight[1,*]

[1]Craniofacial Development and Stem Cell Biology; King's College London; London, UK; [2]MRC Centre for Developmental Neurobiology; King's College London; London, UK; [3]Department of Cell and Developmental Biology; University College London; London, UK; [4]CoMPLEX; University College London; London, UK

Keywords: axin, GSK-3, IWR-1, mesencephalon, neuron, trigeminal, Tankyrase, zebrafish, β-catenin

Abbreviations: MTN, mesencephalic trigeminal nucleus; nTPC, nucleus of the tract of the posterior commissure; Wnt, wingless related integrated site; FGF, Fibroblast growth factor; CA-fgfr1, constitutively active fgf receptor 1; BIO, 6-bromoindirubin-3′-oxime; IWR-1, Inhibitors of Wnt Response 1; cat, β-catenin; dkk1, dickkopf Wnt signaling pathway inhibitor 1; GSK-3, glycogen synthase kinase; A-P, anterior-posterior; GFP, green fluorescent protein; hpf, hours post fertilization; dpf, days post fertilization.

Interactions between FGF and Wnt/ bcat signaling control development of the midbrain. The nature of this interaction and how these regulate patterning, growth and differentiation is less clear, as it has not been possible to temporally dissect the effects of one pathway relative to the other. We have employed pharmacological and genetic tools to probe the temporal and spatial roles of FGF and Wnt in controlling the specification of early midbrain neurons. We identify a β-catenin (bcat) independent role for GSK-3 in modulating FGF activity and hence neuronal patterning. This function is complicated by an overlap with bcat-dependent regulation of FGF signaling, through the regulation of sprouty4. Additionally we reveal how attenuation of Axin protein function can promote fluctuating levels of bcat activity that are dependent on FGF activity. This highlights the complex nature of the interactions between FGF and Wnt/ bcat and reveals that they act at multiple levels to control each others activity in the midbrain.

Introduction

The control of neurogenesis is critical for ensuring the correct number of neurons form at the appropriate place during development and regeneration. Disruption to this process occurs in a number of congenital disorders that result in cognitive impairment.[1] Signaling pathways play a critical role in controlling where and when neurons form, so are presumed to be robustly regulated, to ensure that fluctuations of any one pathway are buffered and do not perturb neurogenesis. Buffering of signaling pathway activity is achieved through regulatory interactions between pathways, that act to limit or promote activity, for instance by controlling expression of ligands or the activity of activators or repressors. The interaction between Wnt and FGF signaling in the developing midbrain is a well-explored example of this interplay between 2 critical pathways.[2,3]

FGF and Wnt Regulation of Neurogenesis

The isthmus arises at the midbrain-hindbrain boundary and acts as an organizer for adjacent tissues.[3,4] In the midbrain, FGFs secreted from the isthmus controls the patterning of the midbrain and anterior hindbrain.[5-10] At later stages, FGF activity controls the onset of neurogenic differentiation across the midbrain[11,12] and acts to specify dopaminergic and serotenergic neurons in the ventral midbrain.[13-15] Changes to midbrain identify in animals showing reduced levels of FGF signaling are presumed to reflect a key role of FGFs in specifying regional fate in the midbrain. Specifically, mice or zebrafish with loss of function of Fgf8 show hyoplastic midbrain and anterior hindbrain.[16,17]

The canonical Wnt signaling pathway activates the nuclear transcription co-factor β-catenin (bcat) and is important for multiple aspects of neuronal development. It is known to be important for regulating cell proliferation through the cell cycle regulator cyclinD1 and c-myc and perturbations to Wnt affect midbrain size.[18-23] Wnt/ bcat signaling is also a regulator of neurogenesis and induces expression of *Neurogenin1, Neurogenenin2* and *NeuroD1*.[24,25] Both early specification and later differentiation of dopaminergic neurons in the ventral midbrain are regulated by Wnt/ bcat signaling.[26-30]

*Correspondence to: Robert D Knight; Email: robert.knight@kcl.ac.uk
Submitted: 03/07/2014; Revised: 05/07/2015; Accepted: 05/27/2015
http://dx.doi.org/10.1080/23262133.2015.1057313

Cross-Talk between Wnt and FGF

A well-characterized regulatory feedback loop operates to maintain *Wnt1* and *Fgf8* expression at the isthmus.[2] Manipulations of Wnt or FGF signaling in chick embryos have revealed that both pathways are required for activity of the other.[31] However, it is unclear if there is a hierarchy of events in which one pathway controls the others and whether they alter the biological responses of each other. Computational modeling of the spatial expression of Wnt and FGF signaling pathway genes in mutant mice has suggested that FGF signaling is required for the maintenance of *Wnt1* expression at the isthmus, but not induction.[32] A number of studies reveal that Wnts and FGFs have multiple roles during midbrain development and neurogenesis, independent of their role in conferring regional patterning. In cortical neurons, bcat acts to promote neuronal differentiation and can override FGF signals that promote proliferation, by inducing expression of the pro-neurogenic factor Neurogenin1.[24] Neural stem cells likewise respond differently to Wnt and FGF signaling dependent on whether both signals are present. In the presence of FGF2, bcat promotes neural stem cell proliferation; in an absence of FGF2 bcat promotes neuronal differentiation.[33] Thus an interplay between Wnt and FGF regulates both neuronal progenitor proliferation, but also differentiation. The balance of these respective roles is therefore critical for orchestrating growth of the developing brain and ensuring that appropriate neuronal populations form in the correct sites.

We have previously investigated how development of early forming dorsal brain neurons are regulated by FGF and Wnt signaling.[34] Using a combination of pharmacological and genetic manipulations we found that positioning and number of mesencephalic trigeminal nucleus (MTN) neurons is dependent on the level of FGF and Wnt activity. We and others have shown that FGF signaling from the isthmus controls neuronal differentiation in the midbrain, through regulation of Hairy-related genes *her5* and *him*.[8,35,36] A posterior retraction of *her5* expression toward the isthmus controls where and when neuronal differentiation occurs in the midbrain.[37] Using *pea3* as a readout of FGF activity, we postulated this corresponds to a gradient of FGF signaling that is retracting posteriorly in the midbrain during development.[34] We investigated the interaction of FGF and Wnt in controlling this process by applying inhibitors of FGF receptors (SU5402) and GSK-3 (BIO). This revealed that FGF signaling is GSK-3 dependent and that the FGF receptor inhibitor *sprouty4* is regulated by Wnt signaling. It is important to understand the nature of these interactions because of their potential impact on the spatiotemporal control of neurogenesis in the brain. We have therefore investigated the role of Wnt/ bcat activity in controlling development of MTN neurons in the midbrain and how the interaction with FGF signaling affects this process.

In this work, we identify an interaction between GSK-3 and FGF intracellular signaling pathways, independent of the Wnt/ bcat pathway. Specifically we note that attenuation of Wnt/ bcat signaling or of Axin function do not alter positioning of MTN neurons, in contrast to an inhibition of GSK-3 function. Furthermore, FGF responsive genes are affected differently by bcat overexpression and manipulation of GSK-3. Intriguingly, we find that bcat-regulated genes do not respond in a linear manner to Axin protein levels, suggesting that feedback loops act to modulate the output of Wnt/ bcat during midbrain development.

Methods

Animals and embryo manipulations

All experiments were performed in accordance with UK Home Office regulations. Embryos were grown at 28.5°C as previously described.[38] Lines used were AB (considered to be wild-type), *masterblind* (mbl),[39], *Tg[elavl3:gfp]*,[40] *Tg[dusp6:d2eGFP]*,[41] *Tg[hsp70l:dkk1b-gfp]*,[42] *Tg[hsp70:ca-fgfr1]*,[43] *Tg[hsp70:gal4]*,[44] *Tg[dlx5a/6a:eGFP]*,[45] *Tg[UAS:HA-β-catenin]*,[34] *Tg[TOPdGFP]*.[46]

Heat shock induction was performed by moving embryos to 37°C for 2 hours at 16.5 hours post fertilization (hpf). Pharmacological treatments were performed by applying either SU5402 (Sigma), BIO (Invitrogen) or IWR-1 (Merck) diluted in embryo medium as previously described.[34] For all experimental conditions, a minimum of $n = 10$ embryos were used; for each individual experiment containing multiple conditions, embryos from the same clutch were used to minimise variation in developmental stage.

In situ hybridization and Immunohistochemistry

Gene expression was visualised by *in situ* hybridization and proteins detected by immunohistochemistry as previously described.[47,48] Antibodies used were anti-HuC/D (1 : 500, Invitrogen), anti-Isl1 (1 : 200, DSHB), anti-acetylated tubulin (1 : 200, Sigma), anti-GFP (1 : 500, AMS Biotechnology), anti-HA (1 : 300, Roche). Back labeling of axons was performed by applying DiI or DiD to muscles of fixed 5 dpf larvae using a sharpened tungsten needle. Fluorescent images were acquired using a Nikon C-1 Eclipse confocal microscope and processed using Photoshop (Adobe).

Mathematical modeling

Statistical models and analyses were generated using the R programming language (R Development Core Team, 2010) as described previously.[34] A minimum of 10 measurements were used for each condition in each experiment. The models used tested variables across a number of datasets and assessed batch effects for significance.

The model of Lee et al.[49,50] describing Wnt signaling and bcat activity was converted into equivalent code for the Python programming language. Under the assumption that degradation of Axin (reaction 15 in the original model, described by the rate constant $k1_5$) is primarily through its ubiquitination by Tankyrase, this model was then simulated under varying values of k_{15} (other rates were kept as in the original model description).

Results

FGF signaling controls positioning and number or early forming midbrain neurons

We have previously identified MTN neurons in the anterior midbrain by retrograde labeling of adductor mandibulae muscles using DiI.[34] In order to ascertain whether MTN neurons also innervate other cranial muscles, we labeled *lateral rectus* and *levator arcus palantini* muscles with DiD and *adductor mandibulae* muscle with DiI in 5 day post fertilization (dpf) larvae. We found that MTN neurons were back labeled with both DiD and DiI, but all labeled MTN neurons were restricted to the anterior midbrain, as we have found previously (**Fig. 1A**). To understand why MTN neurons arise in the anterior midbrain, we used a transgenic line that labels developing neurons in the developing brain. The *elavl3* gene encodes the HuC protein, a marker of differentiated neurons.[40] At 24 hpf, GFP expressing (GFP+) neurons in *Tg[elavl3:eGFP]* embryos are observed in the dorsal brain, in the nucleus of the posterior commissure (nTPC) and in the anterior midbrain. GFP+ MTN neurons undergo differentiation in an anterior-posterior manner from 22 hpf as shown by the presence of HuC protein (**Fig. 1B**). Treatment with the FGF receptor antagonist, SU5402, at stages prior to MTN differentiation, leads to an increased number of MTN neurons that lie at more posterior positions along the midbrain, relative to control animals (**Fig. 1C**).[34] This suggests that FGF signaling controls where MTN neurons will form in the midbrain during development. Isl1 is expressed by all primary neurons in the developing zebrafish brain.[51] To determine whether FGF signaling is active in the anterior midbrain where MTN neurons will first differentiate, we labeled MTN neurons by an anti-Isl1 antibody and compared to GFP localization in a reporter line for FGF signaling that expresses GFP under the control of the *Dusp6* promoter (*Tg[dusp6:d2GFP]*). Strikingly, there was no co-localization of GFP and Isl1 revealing that MTN neurons differentiate in regions devoid of FGF signaling (**Fig. 1D–I**). Commensurate with this, *fgfr1* is not expressed in anterior midbrain cells at this stage, suggesting that cells are not able to respond to FGF signaling (**Fig. 1J**). We wished to know whether a temporal inhibition of FGF signaling during stages prior to MTN formation would affect the development of later-forming neuronal populations in the midbrain including the optic tectum. To investigate this, embryos were treated from 14–24 hpf with SU5402 or DMSO, then drug washed away and embryos allowed to develop until 30 hpf. In SU5402 treated embryos we observed more posteriorly located MTN neurons in the midbrain and a smaller optic tectum (**Fig. 1K and L**). Thus, a temporal inhibition of FGF signaling at stages when primary neurons form, leads to perturbations of midbrain neuronal architecture.

Wnt/ bcat signaling interacts with FGF to direct MTN formation

The well documented interaction between FGF and Wnt/ bcat signaling suggests that manipulations of bcat activity would also affect positioning of MTN neurons. We therefore compared how alterations of Wnt relative to FGF signaling affected the positioning of MTN neurons. MTN neuron positioning relative to the isthmus was quantified in 24 hpf embryos under the following conditions: 1) expression of a constitutively active FGF receptor (CA-Fgfr1), 2) application of SU5402, 3) expression of the Wnt antagonist dickkopf1b (dkk1), 4) application with BIO. All manipulations were performed between 14–24 hpf (SU5402, BIO) or 16.5–24 hpf (CA-Fgfr1, dkk1) as we have previously shown that MTN, but not adjacent diencephalic neurons, are sensitive to manipulations of FGF and Wnt signaling at this stage.[34] The position of the most posteriorly located MTN neurons in the midbrain was measured relative to the isthmus for each condition and expressed as a ratio relative to the midbrain size to compensate for any differences in size. This revealed that over-activation of FGF resulted in an anterior shift of MTN neurons (**Fig. 2A**). In contrast, SU5402 treated embryos displayed posteriorly located MTN neurons relative to controls (**Fig. 2B**). BIO treatment caused a similar phenotype to SU5402 treatment, with MTN neurons present at more posterior positions in the midbrain (**Fig. 2C**). In contrast, abrogation of Wnt signaling by overexpression of dkk1 had no effect on MTN positioning (**Fig. 2D**). This suggests that the posterior displacement of MTN neurons observed in BIO treated embryos may reflect a role for GSK-3 in controlling neuronal differentiation along the dorsal midbrain, independent of its role in regulating Wnt signaling.

GSK3 and bcat differentially regulate FGF signaling in the midbrain

The different changes to neuronal pattering caused by altering Wnt and FGF activity suggests that they do not interact in a simple feedback loop to control neurogenesis in the midbrain. To understand the importance of GSK-3 in mediating interactions between Wnt and FGF, we compared the responses of FGF signaling genes to alterations of GSK-3 and bcat activity. Previously, we showed that BIO treatment up-regulates *fgf8a* expression at the isthmus. To determine whether FGF-dependent genes such as *fgf8a* are regulated by GSK-3 or bcat activity, the affects of GSK-3 inhibition or bcat over-expression were compared when FGF signaling was attenuated using the inhibitor SU5402. Embryos were treated with 10μM SU5402 from 14 hpf in the presence of varying doses of BIO or a stabilised HA tagged bcat. Expression of *fgf8a* at the isthmus was assessed at 24 hpf by *in situ* hybridization and found to be down-regulated by SU5402 treatment (**Fig. 3A and B**). In contrast, BIO causes elevated *fgf8a* expression compared to controls (**Fig. 3C**). Surprisingly, in the presence of both BIO and SU5402 *fgf8a* expression was higher than in embryos treated with BIO alone (**Fig. 3D**). Overexpression of bcat resulted in reduced *fgf8a* expression, unlike BIO treatment (**Fig. 3E and F**). In the presence of SU5402, overexpression of bcat then rescued *fgf8a* relative to embryos treated with SU5402 alone (**Fig. 3G and H**). These results were consistent between embryos (see also **Fig. S1**) and reveal that *fgf8a* responds differently to BIO treatment and bcat overexpression. However, both BIO and bcat over-expression are able to rescue *fgf8a* expression in the presence of SU5402.

To show how *fgf8a* responses compare to a transcriptional read-out of FGF activity we assessed the response of the ETS

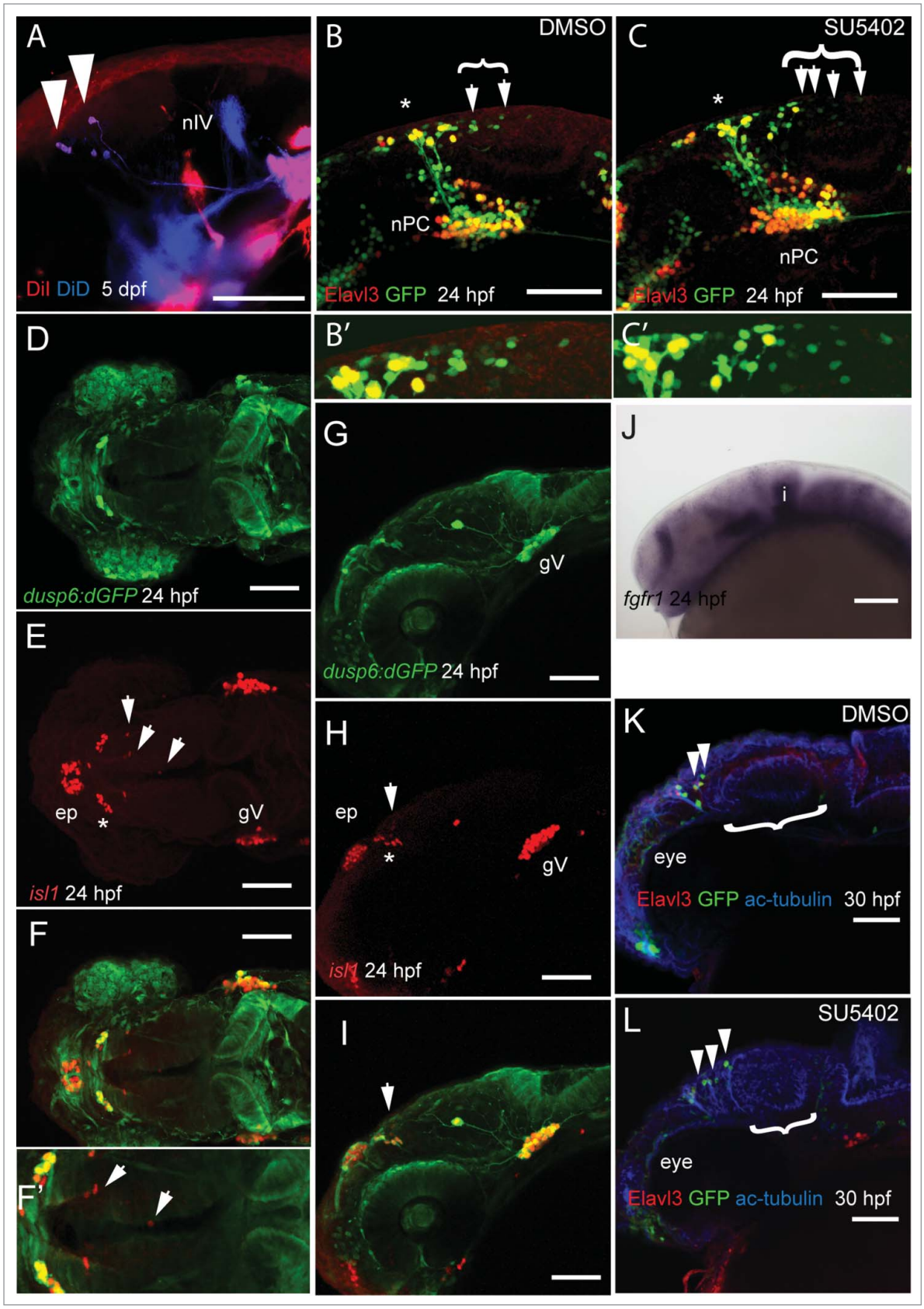

Figure 1. For figure legend, see page 5.

family gene *pea3* at the isthmus and midbrain signaling under different levels of FGF, GSK-3 and bcat activity. Both SU5402 and BIO treatment cause a reduction of *pea3* expression (**Fig. 3I–K**). SU5402 was used at 6μM in combination with BIO as higher SU5402 concentrations (10μM) lead to a loss of *pea3* expression, precluding quantification. In the presence of SU5402, BIO caused a further reduction of *pea3* expression than when treated with BIO or SU5402 alone (**Fig. 3L**).

Overexpression of bcat also leads to a reduction of *pea3* expression, similar to BIO (**Fig. 3M and N**). In contrast to BIO, over-expression of bcat in the presence of SU5402 does not further repress *pea3* (**Fig. 3O and P**, see also **Fig. S2**). These differential responses of genes in the FGF signaling pathway to BIO and bcat overexpression suggests that GSK-3 affects FGF signaling in a bcat-independent manner (**Table 1**).

Wnt responsive genes are affected differently by changes to β-catenin and GSK-3 activity

GSK-3 may also regulate Wnt signaling independently of its role in inhibiting β-catenin activity in the bcat destruction complex (bcatDC). To test this we investigated how genes in the Wnt pathway are affected by inhibiting FGF signaling in conjunction with GSK-3 inhibition compared to bcat over-expression. Application of SU5402 or BIO leads to reduced *wnt1* expression (**Fig. 4A–C**). Application of BIO in presence of SU5402 causes a further inhibition of *wnt1* (**Fig. 4D**). In contrast to the response of *wnt1* to BIO treatment, *wnt1* is up-regulated by overexpression of bcat (**Fig. 4E and F**). Application of SU5402 abrogates this response (**Fig. 4G and H**, see also **Fig. S3**). This reveals a differential response of *wnt1* to inhibition of GSK-3 and elevated β-catenin activity, suggesting that GSK-3 has a bcat-independent function in controlling *wnt1* expression.

To determine how GSK-3 inhibition or bcat over-expression can affect Wnt/ bcat activity, we used *lef1* as a transcriptional readout. SU5402 treatment results in down-regulation of *lef1* (**Fig. 4I and J**). In contrast, inhibition of GSK-3 by BIO results in a slight up-regulation of *lef1* expression (**Fig. 4K**). In the presence of SU5402 and BIO, *lef1* expression was strongly upregulated (**Fig. 4L**). This upregulation was much greater than in embryos treated with BIO alone, implying that GSK-3 inhibition causes a much stronger activation of bcat when FGF signaling is likewise inhibited. We then evaluated how overexpression of bcat affects *lef1* expression. As predicted, bcat over-expression causes an up-regulation of *lef1* (**Fig. 4M and N**). In the presence of SU5402, bcat overexpression can rescue *lef1* expression (**Fig. 4O and P**, see also **Fig. S4**).

In summary, we found that *lef1* expression is reduced by SU5402, indicating a requirement for FGF activity to promote bcat signaling. Both BIO and bcat can rescue this reduction in the presence of SU5402, suggesting bcat regulation of *lef1* is not dependent on FGF activity.

Inhibition of Wnt signaling does not affect MTN neuron positioning in the midbrain

To further probe the relative roles of Wnt and FGF signaling in controlling each others activity, we focused on the role of the key regulator of the bcat destruction complex, Axin. We have previously described how IWR-1 acts in an antagonistic manner to SU5402 to control the number of MTN neurons that form.[34] Inhibition of Wnt signaling (by over-expression of dkk1) does not affect MTN positioning (**Fig. 2D**). We therefore tested whether stabilization of Axin, through inhibition of Tankyrase, would affect MTN positioning in the midbrain. Although application of varying IWR-1 doses resulted in the formation of fewer MTN neurons (**Fig. 5A**) there was no effect on the distance of MTN neurons to the isthmus (**Fig. 5B**). A comparison of MTN neuron number relative to the MTN-isthmus distance showed no correlation when embryos were exposed to IWR-1 in the presence of SU5402 (**Fig. 5C**). We than asked whether changes to the MTN-isthmus distance in embryos exposed to IWR-1 and SU5402 could be explained by the application of either IWR-1 or SU5402. We find that there is no correlation bewteen MTN neuron number and distance to the isthmus in embryos exposed to both IWR-1 and SU5402 ($R = 0.028$, **Fig. 5D**). Two-way ANOVA tests revealed that IWR-1 had no significant affect ($p = 0.616$) on MTN neuron positioning, but SU5402 had a strong affect ($p = 0.0012$). Moreover, there is no interaction effect expected if IWR-1 and SU5402 are acting synergistically or antagonistically ($p = 0.839$). In contrast, models that describe MTN neuron number revealed that there is both a strong IWR-1 affect ($p = 1.23 \times 10^{-6}$, **Table 2**) and a strong interaction effect between IWR-1 and SU5402 ($p = 0.0048$, **Table 2**). These models indicate that although inhibition of Tankyrase results in fewer MTN neurons, this does not occur in conjunction with posterior shifts of MTN neurons observed following abrogation of FGF activity (by SU5402) or inhibition of GSK-3 (by BIO). Loss of Wnt signaling by overexpression of dkk1 likewise causes a decrease in the number of MTN neurons forming, but this does not correlate with altered positioning within the midbrain

Figure 1 (See previous page). FGF signaling dictates the spatial positioning of MTN neurons in the midbrain during development. DiI (red) labeling of masseter and and DiD (blue) labeling of levator arcus palatini and lateral rectus cranial muscles in 5 dpf larvae leads to retrograde labeling of MTN neurons in the anterior midbrain (**A**). Lateral views of *Tg[elavl3:egfp]* embryos labeled with anti-GFP (green) and anti-Elavl3 (HuC/D, red) reveals the presence of more MTN neurons (arrowheads) at posterior locations in the midbrain following treatment with 40μM SU5402 from 14–24 hpf (**C**) relative to DMSO exposure (**B**). Bracket indicates extent of MTN neurons (represented by enlarged area in B′ and C′). Dorsal (**D–F**) and lateral (**G–I**) views of 24 hpf *Tg[dusp6:d2eGFP]* embryos processed with anti-GFP (green) and anti-Isl1 (red). A zoomed dorsal view (**F′**) reveals that neurons of the nucleus of the tract of the posterior commissure (nTPC, asterisk) and MTN neurons (arrowheads) develop in regions devoid of anti-GFP labeling. At 24 hpf, *fgfr1* expression is absent from the anterior midbrain (**J**). Lateral views of 30 hpf *Tg[dlx5a/6a:eGFP]* embryos labeled with anti-Elavl3 (red), anti-acetylated tubulin (blue) and anti-GFP (green) reveals more MTN neurons (arrowheads) and a reduced optic tectum (bracket) following exposure to 40μM SU5402 (**L**) from 14–24 hpf compared to DMSO treated control animals (**K**). Nucleus of the posterior commissure (nPC), trochlear nerve (nIV). Scale bars: 50μm (**A**), 100μm (**B–L**).

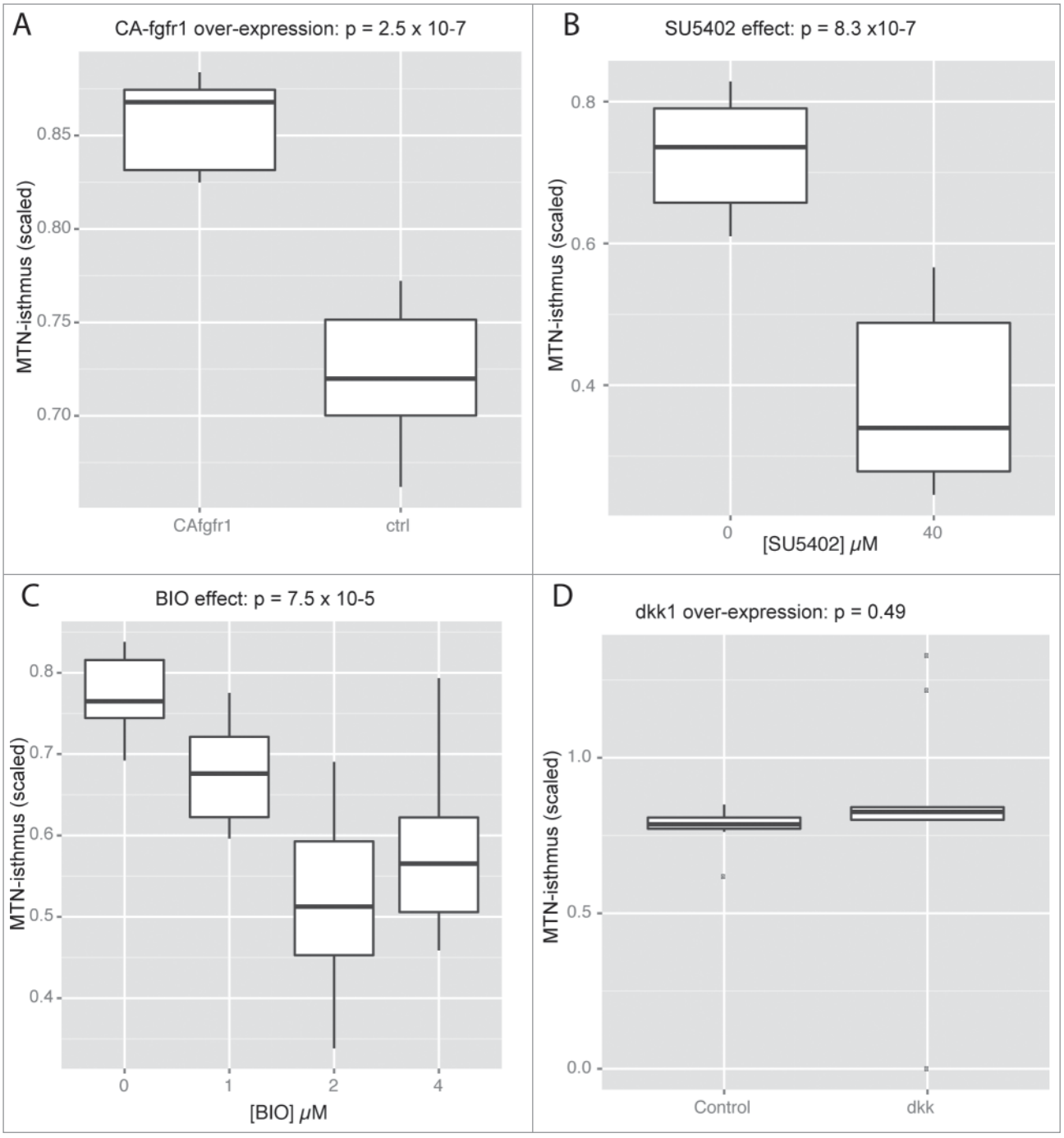

Figure 2. MTN A-P positioning along the dorsal midbrain is regulated by FGF and GSK-3 activity, but does not require Wnt signaling. Box plots representing the minimal distance between MTN neurons and the isthmus scaled relative to midbrain size for embryos expressing CA-fgfr1 (**A**), exposed to 0 or 40μM SU5402 (**B**), exposed with 0, 1, 2, 4μM BIO (**C**), or expressing dkk1b (**D**). Significance was determined by t-test with Welch correction (**A, B, D**) or by a Kruksal-Wallis test (**C**) by comparing to embryos not expressing transgenes or treated only with DMSO carrier (0μM). N = 10 for each condition.

(R = 0.48, **Fig. 5E**). This suggests that inhibition of Wnt signaling by either dkk1 over-expression or IWR-1 application does not perturb the positioning of MTN neurons.

The Hairy-related gene *her5* controls the spatiotemporal onset of neurogenesis in the midbrain and hence where MTN neurons form.[8,35] The expression of *her5* along the A-P extent of the dorsal midbrain is controlled by GSK-3 and FGF activity.[34] To determine whether *her5* shows differential responses to IWR-1 over time, we measured the spatial expression of *her5* at 16.5, 18 and 20 hpf after application of IWR-1 at 14 hpf. We found that no significant changes to *her5* expression occurred initially after exposure to IWR-1, although by 18 hpf the *her5* expression was

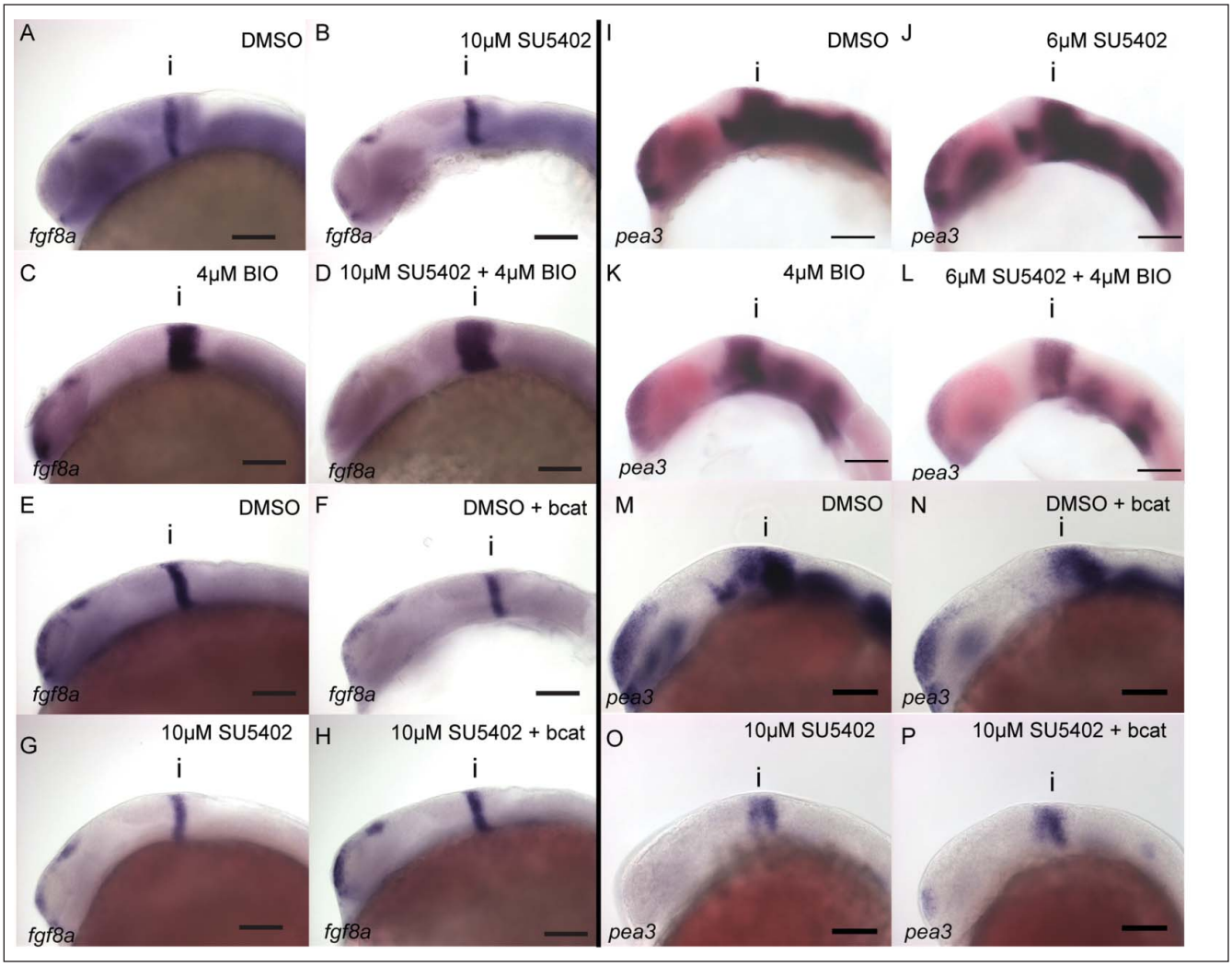

Figure 3. FGF activity in the midbrain is GSK-3 dependent, but is not regulated by β-catenin. Expression of *fgf8a* (**A–H**) and *pea3* (**I–P**) was visualized by *in situ* hybridization in 24 hpf embryos treated with DMSO (**A, E, I, M**), SU5402 at 10μM or 6μM (**B, G, J, O**), BIO at 4μM (**C, K**), SU5402 and BIO together (**D, L**), when over-expressing bcat (**F, N**), when over-expressing bcat and treated with SU5402 (**H, P**). Isthmus (i). Scale bars: 100μm.

reduced relative to control embryos (**Fig. 5F–J**). However, by 24 hpf, there no longer an effect of IWR-1 treatment on *her5* expression in the midbrain.

Having shown that *her5* is not significantly affected by IWR-1, we then tested if inhibition of Wnt signaling would affect the response of *her5* to FGF activity. IWR-1 and SU5402 were applied simultaneously at 14 hpf and the spatial expression of *her5* measured along the dorsal midbrain at 24 hpf. Plots of *her5* expression revealed that IWR-1 did not alter the response of *her5* SU5402 (**Fig. 5K**). We confirmed this by generating models for the response of *her5* to IWR-1 and SU5402 (**Table 3**). These revealed that application of IWR-1 did not have a significant affect on *her5* ($p = 0.322$). In contrast, SU5402 had a significant effect ($p = 0.000282$). Furthermore, IWR-1 did not significantly alter the response of *her5* to SU5402 ($p = 0.0763$). This reveals that bcat activity is not required for the response of *her5* to FGF activity and so does not control the A-P position of MTN neurons in the dorsal midbrain, unlike GSK-3.

bcat activity responses to IWR-1 are not linear relative to dose or time of exposure

Our observation that IWR-1 application caused a transient decrease in *her5* expression led us to wonder whether it caused repression of bcat activity in a dose-dependent and uniform manner. We therefore used expression of *lef1* in the midbrain as a readout of bcat activation and compared embryos treated with IWR-1 at varying doses (20, 30, 40μM) from 14 hpf after 2.5 (16.5 hpf), 4 (18 hpf) and 6 (20 hpf) hours of exposure. Intriguingly, we found that *lef1* responses were affected more by application of 20μM IWR-1 than either 30 or 40 μM after 2.5 hours post application (**Fig. 6A–D**). At later stages this changes, until by 12 hours post application *lef1* is most strongly reduced in embryos treated with the higher doses of 30 and 40μM (**Fig. 6E–L**). Why *lef1* should be more affected by a lower, rather than higher dose of IWR-1 initially is unclear. Expression of *wnt1* at the isthmus is responsive to BIO and bcat activity

Table 1. Summary of gene expression changes in the midbrain at 24 hpf due to alterations of Wnt or FGF activity from 14 hpf (SU5402, IWR-1, BIO) or 16.5 hpf (dkk1, βummar

Signaling pathway manipulation			gene expression in the midbrain					
Wnt	**FGF**	**treatment**	**lef1**	**wnt1**	**pea3**	**her5**	**spry4**	**fgf8**
↑		BIO	↑	↓	↓	↓	↑	↑
↑		bcat	↑	↑	↓	↓	↑	↓
↓		dkk1	↓		↓	↓	↓	
↓		IWR-1	↓	↑		↓		
	↑	CA-fgfr1	↑	↑	↑		↑	↓
	↓	SU5402	↓	↓	↓	↓	↓	↓
↑	↓	BIO + SU5402	↑	↓	↓	↓	↑	↑
↑	↓	bcat + SU5402	↑	↓	↓	↓		
↓	↓	IWR-1 + SU5402	↓	↓	↓	↓	↓	

reduced expression relative to control
no change relative to control
elevated expression relative to control

(**Fig. 4**). We found that the lowest dose of IWR-1 tested (10μM), resulted in the strongest downregulation of *wnt1* expression (**Fig. 6M–P**). We then turned to an alternative reporter of Wnt/ bcat activity, the *Tg[TOPdGFP]* transgenic line, to determine if these responses of *lef1* represent Wnt activity. In this transgenic line, we were unable to discriminate any differences in bcat activity when treated at different IWR-1 doses (**Table 1**, data not shown). This may reflect the relative insensitivity to changes in Wnt signaling levels previously reported.[52] We therefore examined other readouts of bcat activity to determine how they responded to different concentrations of IWR-1 over time.

Previously, we found that the FGF receptor inhibitor, *sprouty4* (*spry4*) shows a dual response to FGF and Wnt/ GSK-3 activity in the midbrain.[34] Strikingly, we noted that *spry4* is sensitive to the level of bcat activity independently from FGF activity. We therefore measured the response of *spry4* to varying doses of IWR-1 from 14 hpf, to determine how similar its response was to that of *lef1*. As observed for *lef1*, expression of *spry4* was

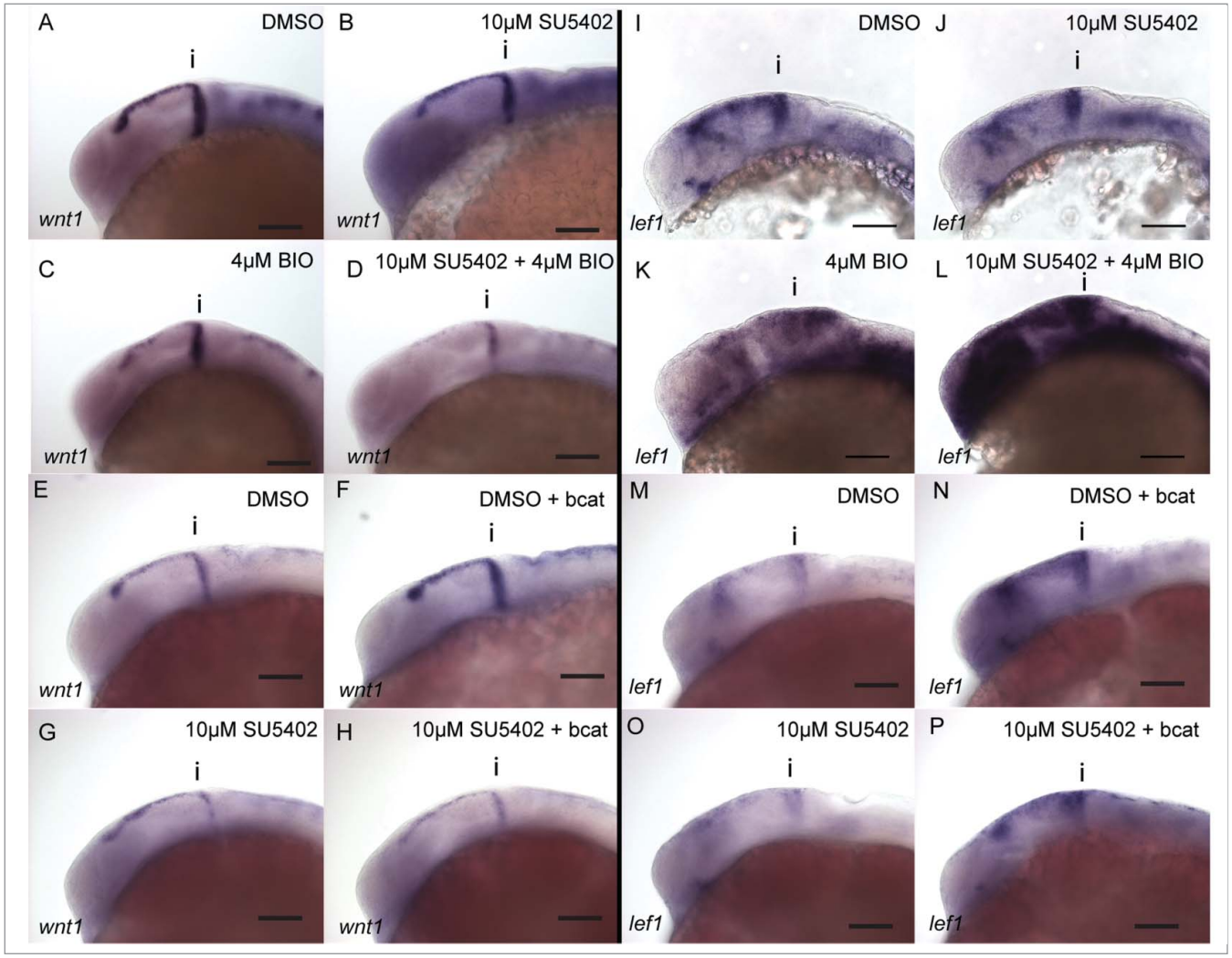

Figure 4. *wnt1* in the midbrain is GSK-3 dependent, but is not regulated by β-catenin. Expression of *wnt1* (**A–H**) and *lef1* (**I–P**) was visualised by *in situ* hybridization in 24 hpf embryos treated with DMSO (**A, E, I, M**), SU5402 at 10μM (**B, G, J, O**), BIO at 4μM (**C, K**), SU5402 and BIO together (**D, L**), when over-expressing bcat (F, N), when over-expressing bcat and treated with SU5402 (**H, P**). Isthmus (i). Scale bars: 100μm.

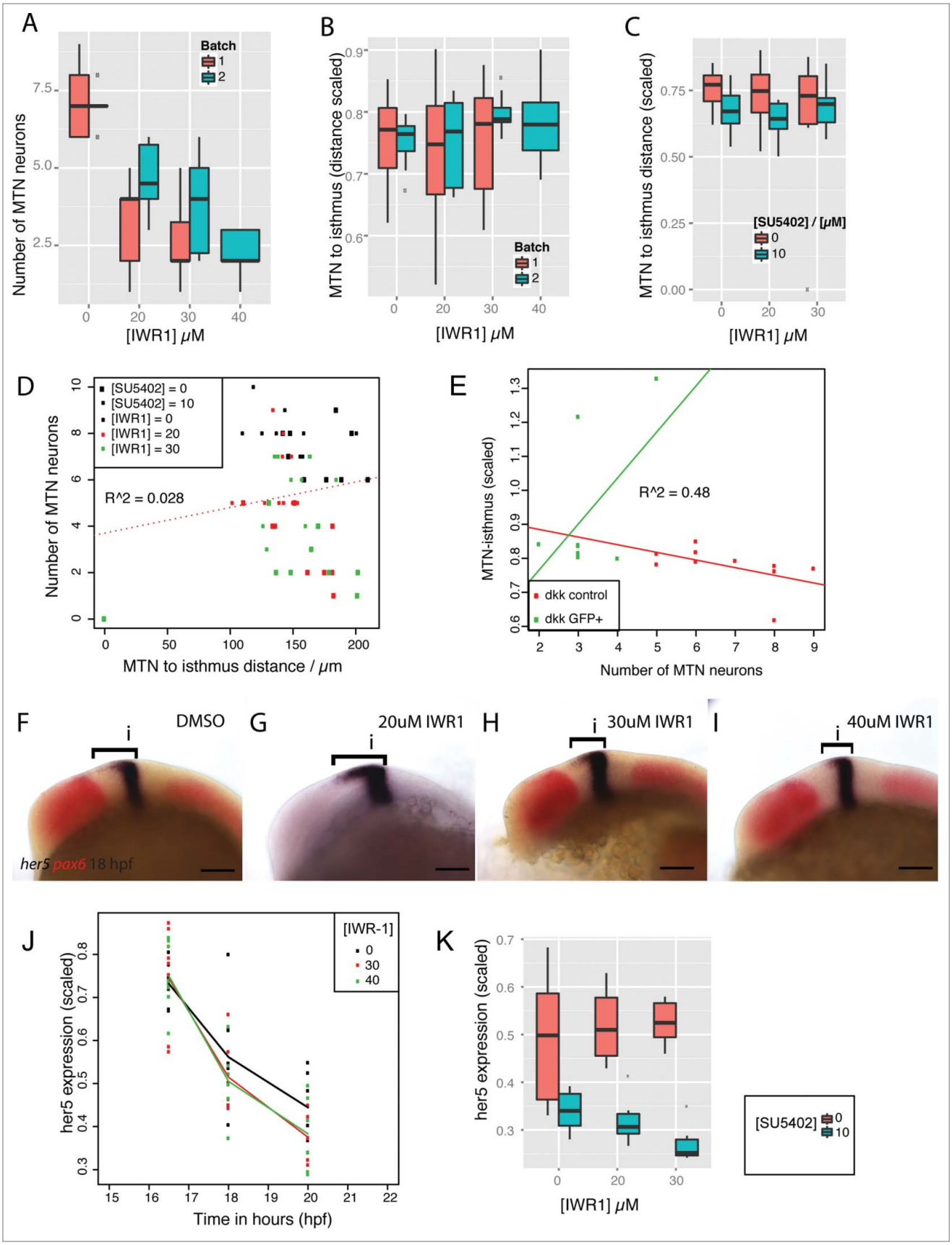

Figure 5. For figure legend, see page 11.

Table 2. Results from Poisson models describing MTN neuron numbers as a function of SU5402 at 10μM (δ([SU5402],10) and IWR-1 at 20 (δ,([IWR120], 20) or 30μM (δr 3IWR1],30). The baseline number of MTN neurons is represented by μ and interactions represented by *d*. Addition of IWR-1 at 20 or 30μM results in significant changes to MTN neuron number ($p<0.001$), but SU5402 at 10μM does not ($p > 0.05$). Application of both SU5402 and IWR-1 results in significant changes to MTN neuron numbers that cannot be explained by simply additive effects, but rather represent interaction effects e.g. $d_{\text{IWR1}=20\ \&\ \text{SU5402}=10}$.

$$y \approx \mu_{Intercept} +$$
$$\delta\left([\text{IWRI}],20\right)\cdot d_{\text{IWRI}=20} + \delta\left([\text{IWRI}],30\right)\cdot d_{\text{IWRI}=30} +$$
$$\delta\left([\text{SU5402}],10\right)\cdot d_{\text{SU5402}=10} +$$
$$\delta\left([\text{IWRI}],20\right)\cdot\delta\left([\text{SU5402}],10\right)\cdot d_{\text{IWRI}=20\,\&\,\text{SU5402}=10} +$$
$$\delta\left([\text{IWRI}],30\right)\cdot\delta\left([\text{SU5402}],10\right)\cdot d_{\text{IWRI}=30\,\&\,\text{SU5402}=10}$$

	Estimate Std.	Error	z value	Pr(>|z|)
(Intercept)	1.9617	0.1250	15.693	< 2e-16
f(IWR1)20	−0.7916	0.2238	−3.536	0.000406
f(IWR1)30	−1.2197	0.2515	−4.850	1.23e-06
f(SU5402)10	0.1316	0.1712	0.768	0.442269
f(IWR1)20:factor(SU5402)10	0.5066	0.2832	1.789	0.073613
f(IWR1)30:factor(SU5402)10	0.8670	0.3074	2.820	0.004796

initially reduced most strongly when 20μM IWR-1 was applied, compared to 30 or 40μM (**Fig. 7A and B**). Continued exposure to IWR-1 revealed that 20μM had the strongest effect on *spry4*. In contrast, higher doses led to an elevated *spry4* expression 4 hours after application relative to DMSO treated control embryos. After 6 hours exposure, all doses of IWR-1 caused a reduced expression of *spry4*, with the lower dose showing the strongest effect. This difference in the response of *spry4* to low or high doses of IWR-1 suggests that a compensatory feedback loop may operate to promote *spry4* expression in response to reduced bcat activity. A good candidate for this is FGF signaling, as Wnt and FGF signaling interact to maintain the isthmus and promote each others activity.[10,31] We therefore tested if abrogation of FGF activity would alter the dose-dependent response of *spry4* to IWR-1, by simultaneously applying both SU5402 and IWR-1. As before, we noted that application of 20μM IWR-1 caused a more severe reduction of *spry4* that 30μM (**Fig. 7C–E**). Likewise, we observed that 10μM SU5402 caused a reduction, but not abrogation of *spry4* expression (**Fig. 7F**). In the presence of SU5402, the response of *spry4* to different doses of IWR-1 is altered and the 30μM dose causes a stronger reduction than 20μM (**Fig. 7G–H**). This suggests that at higher doses of IWR-1, FGF signaling compensates for reduced bcat activity, by promoting *spry4* expression. It also reveals that small reductions of bcat activity do not induce this feedback response by FGF signaling.

A model of Axin inhibition predicts oscillating bcat activity

We found that Wnt/ bcat responsive genes *lef1* and *spry4* show a non-linear response to IWR-1 and this changes relative to the duration of exposure. One putative explanation for the differential effects of IWR-1 dosage on Wnt-target genes may therefore be due to feedback from FGF signaling to promote elevated bcat signaling. IWR-1 inhibition of Tnk reduces the rate of Axin protein degradation, a key limiting step in the activation of bcat.[53,54]

Table 3. Results from generalized linear models describing expression of her5 (scaled relative to midbrain size) as i) a function of SU5402 at 10μM (fSU540210) and IWR-1 at either 20 or 30μM (fIWR120, fIWR130), or ii) a function of SU5402 at 10μM relative to IWR-1 (fIWR1). Addition of IWR-1 at 20 or 30μM does not result in significant changes to her5 expression ($p > 0.05$), but SU5402 does ($p < 0.001$). Addition of 30μM IWR-1 in the presence of SU5402 has an affect on her5 expression with low significance ($p < 0.1$), but overall IWR-1 does not significantly alter the response of her5 to SU5402 ($p = 0.076$). Fit of data to models $R^2 = 0.67$

i) her5 expression as a function of IWR-1 and SU5402 concentration.

$$y_{\text{her5}} = \beta_{\text{Intercept}} + \begin{cases} \beta_{\text{fIWR120}} \text{ if } [\text{IWR1}]=20 \\ 0 \text{ otherwise} \end{cases} + \begin{cases} \beta_{\text{fIWR130}} \text{ if } [\text{IWR1}]=30 \\ 0 \text{ otherwise} \end{cases} + \begin{cases} \beta_{\text{fIWR120}} \text{ if } [\text{SU5402}]=10 \\ 0 \text{ otherwise} \end{cases} + \begin{cases} \beta_{\text{fIWR120:fSU540210}} \text{ if } [\text{IWR1}]=20 \text{ and } [\text{SU5402}]=10 \\ 0 \text{ otherwise} \end{cases} + \begin{cases} \beta_{\text{fIWR130:fSU540210}} \text{ if } [\text{IWR1}]=30 \text{ and } [\text{SU5402}]=10 \\ 0 \text{ otherwise} \end{cases}$$

	Estimate Std.	Error	t value	Pr(>|t|)
(Intercept)	0.48836	0.02693	18.136	< 2e-16 ***
fIWR120	0.03078	0.03942	0.781	0.440123
fIWR130	0.03709	0.04113	0.902	0.373348
fSU540210	−0.14845	0.03808	−3.898	0.000418 ***
fIWR120:fSU540210	−0.05031	0.05697	−0.883	0.383250
fIWR130:fSU540210	−0.10557	0.05817	−1.815	0.078133.

ii) her5 expression as a function of IWR-1 and SU5402 presence.

$$y_{\text{her5}} = \beta_{\text{Intercept}} + \begin{cases} \beta_{\text{fSU540210}} \text{ if } [\text{SU5402}]=10 \\ 0 \text{ otherwise} \end{cases} + [\text{IWR1}]\cdot\beta_{\text{IWR1}} + [\text{IWR1}]\cdot\begin{cases} \beta_{\text{fSU540210:IWR1}} \text{ if } [\text{SU5402}]=10 \\ 0 \text{ otherwise} \end{cases}$$

	Estimate Std.	Error	t value	Pr(>|t|)
(Intercept)	0.489451	0.025566	19.145	< 2e-16***
fSU540210	−0.145272	0.036210	−4.012	0.000282***
IWR1	0.001297	0.001294	1.003	0.322598
fSU540210:IWR1	−0.003342	0.001833	−1.823	0.076349.

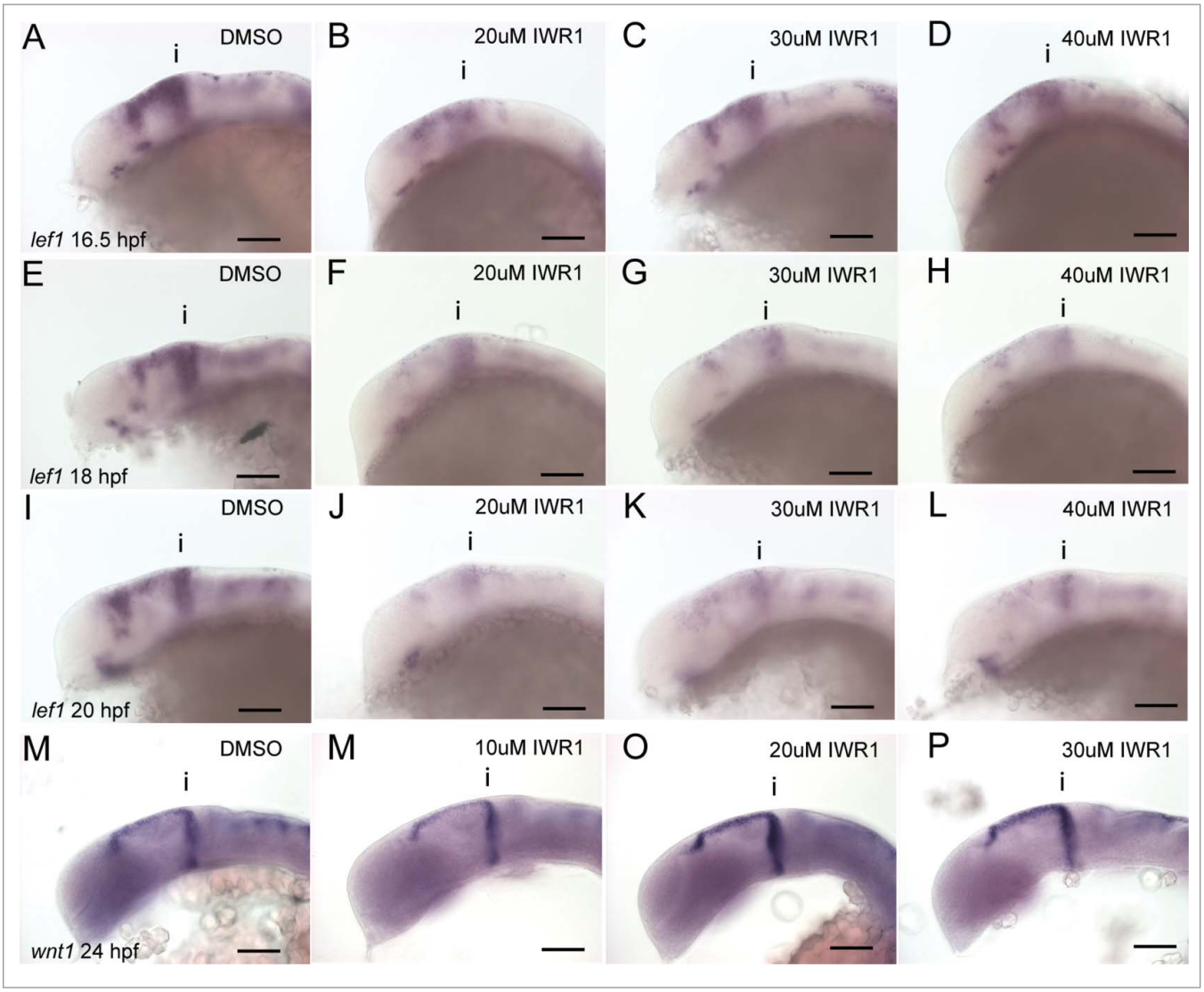

Figure 6. Tankyrase inhibition does not lead to linear reductions of bcat activity over time. Lateral views of 16.5 (**A–D**), 18 (**E–H**), 20 hpf (**I–L**) embryos processed by *in situ* hybridization to reveal expression of *lef1* expression following treatment with IWR-1 at 0, 20, 30, 40 μM IWR-1 from 14 hpf. Lateral views of 24 hpf embryos processed by *in situ* hybridization to reveal expression of *wnt1* expression following treatment with IWR-1 at 0, 20, 30, 40 μM IWR-1 from 14 hpf. Isthmus (i). Scale bars: 100μm.

Figure 5 (See page 9). Tankyrase activity does not affect positioning of MTN neurons or FGF directed *her5* expression in the dorsal midbrain. Box plot of the number of MTN neurons (**A**) or MTN-isthmus distance (scaled by midbrain size, **B**) in 2 separate clutches of embryos (red, blue) treated with 0, 20, 30, 40μM IWR-1 from 14–24 hpf (n = 10 for each condition). Box plot of MTN-isthmus distance (scaled) in 24 hpf embryos treated with DMSO (red) or 10μM SU5402 (blue) in conjunction with IWR-1 (**C**, n = 10 for each condition). Dot plot of MTN neuron number relative to MTN-isthmus distance (scaled) for embryos treated with IWR-1 (0, 20, 30, 40μM) and SU5402 (0, 10μM) from 14 hpf (**D**). A correlation test reveals no correlation between neuron number and distance (R = 0.028, n = 10 for each condition). Dot plot of MTN-isthmus distance (scaled) relative to MTN number in 24 hpf control embryos (red) or *Tg[hsp70l:dkk1b-gfp]* embryos expressing dkk1b (green) from 16.5 hpf (**E**). A correlation test reveals no correlation between MTN neuron number and distance (R = 0.48, n = 10 for each condition). Lateral views of 18 hpf embryos processed by *in situ* hybridization to reveal expression of *her5* (blue, bracket indicates expression extent in dorsal midbrain) and *pax6* (red) following treatment with IWR-1 at 0, 20, 30, 40μM IWR-1 from 14 hpf (**F-I**). A line plot of the *her5* expression domain in the dorsal midbrain (scaled to midbrain size) in embryos treated with IWR-1 at 0, 30, 40μM from 14 hpf at 16.5, 18, 20 hpf (J, n = 10 for each condition). Box plot of *her5* expression domain in the dorsal midbrain (scaled) in 24 hpf embryos treated with IWR-1 at 0, 20, 30μM and SU5402 at 0 (red) and 10μM (blue) from 14 hpf (K, n = 10 for each condition). Isthmus (i). Scale bars: 100μm.

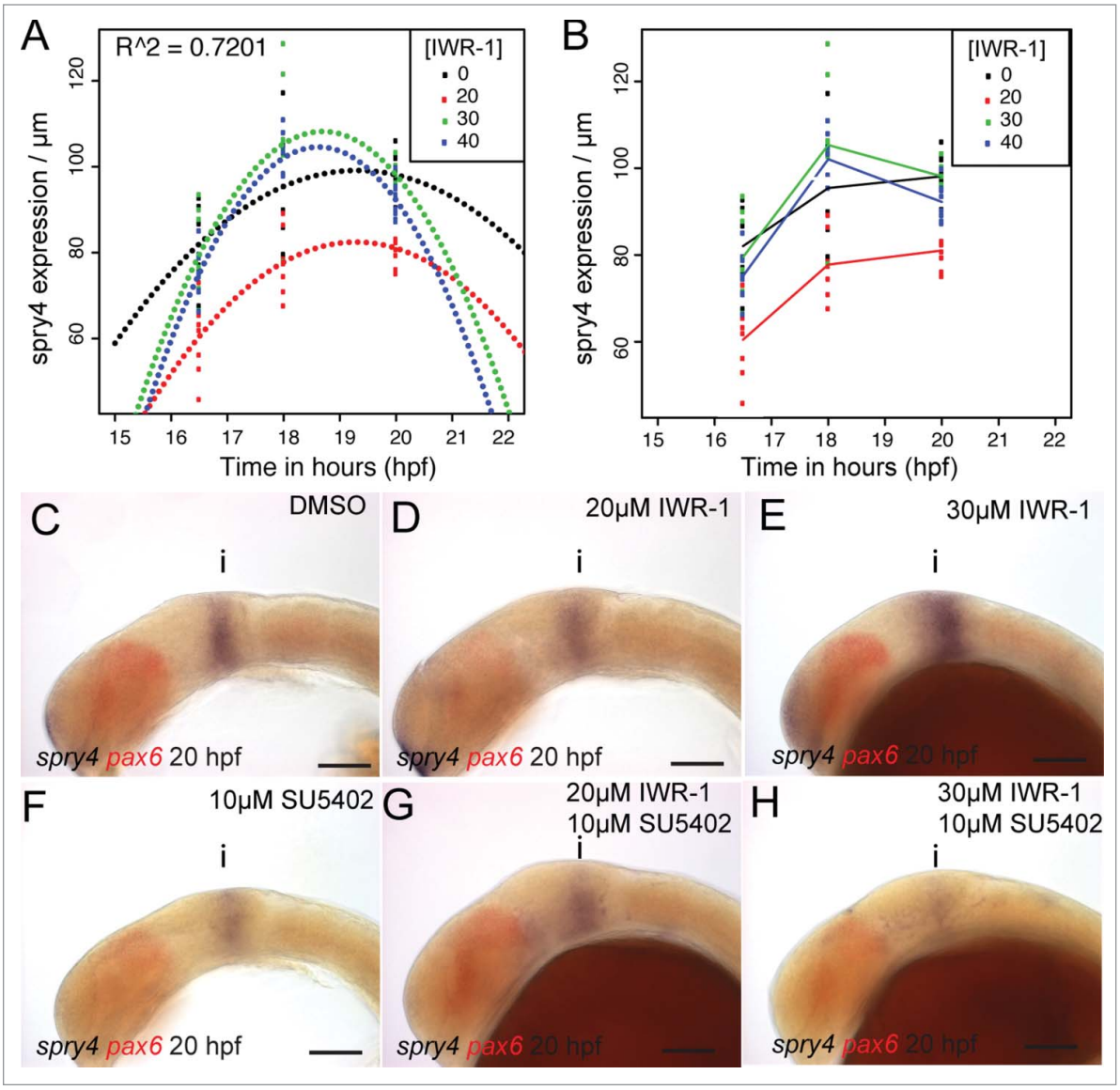

Figure 7. *spry4* shows a bivalent response to changes in Wnt and FGF signaling. Polynomials were fitted against the spatial expression of *spry4* in the dorsal midbrain (µm) at 16.5, 18, 20 hpf following treatment with IWR-1 from 14 hpf (**A**) and showed a good fit ($R^2 = 0.7201$, n = 10 for each condition). A line plot of the *spry4* expression domain (scaled to midbrain size) in the same embryos (**B**) reveals that treatment with 20µM IWR-1 had the strongest affect (n = 10 for each condition). Lateral views of 20 hpf embryos processed by *in situ* hybridization to reveal *spry4* (blue) and pax6 (red) expression following treatment from 14 hpf with DMSO (**C**), 20µM IWR-1 (**D**), 30µM IWR-1 (**E**), 10µM SU5402 (**F**), 20µM IWR-1 with 10µM SU5402 (**G**), or 30µM IWR-1 with 10µM SU5402 (**H**). Isthmus (i). Scale bars: 100µm (C–H).

We used the model of Lee et al[49] to examine how changing the rate at which Axin is ubiquinated by Tnk affects bcat activity. We modified the model such that the Axin degradation term was dependent on the concentration of Tnk:

$$k15[Axin] \rightarrow k15'[Tnk][Axin]$$

Therefore, adding IWR-1 will reduce the contribution of Tnk to the rate (k_{15}) at which Axin is degraded and so decrease this rate overall. A plot of Axin protein relative to different rates of Axin degradation reveals that at high IWR-1 doses (corresponding to low concentrations of Tnk), Axin protein accumulates (**Fig. 8A**). This corresponds with a decrease in free bcat. We wondered how Axin concentration (and thus Tnk activity) was related to bcat concentration in the model and observed a nonlinear response for the bcat, divided into 2 regions (**Fig. 8B**): a flat region corresponding to very low Axin concentrations and an inversely linear region corresponding to higher concentrations, described by the (fitted) power law equation:

$$[bcat] = 0.078[Axin]^{-1.003}$$

This linear region corresponds to Axin concentrations measured from *Xenopus* eggs and used for construction of the

model, hence provides the region most likely occurring in a biological context. An analysis of how free bcat concentration changes relate to induction of a Wnt/ bcat induced phenotype or induction of *siamois* or *Xnr3* in *Xenopus* embryos suggested it is the fold change of free bcat concentration that dictates the response to Wnt signaling.[50,55] Using the same model as above, we investigated how the concentration of bcat changes relative to different rates of Axin degradation prior to and after Wnt stimulation (**Fig. 8C**). As before, high rates of Axin degradation lead to high levels of bcat. We then used this result to ask how the fold change of free bcat is affected by the Axin degradation rate (**Fig. 8D**). Intriguingly, we note that the fold change of bcat is predicted to be relatively high when Axin degradation is high or medium, but that it precipitously drops at low rates of Axin degradation. Our interpretation of this model is that IWR-1 will reduce the levels of free bcat, by promoting elevated levels of Axin, but also allow a greater fold change in bcat levels upon Wnt stimulation.

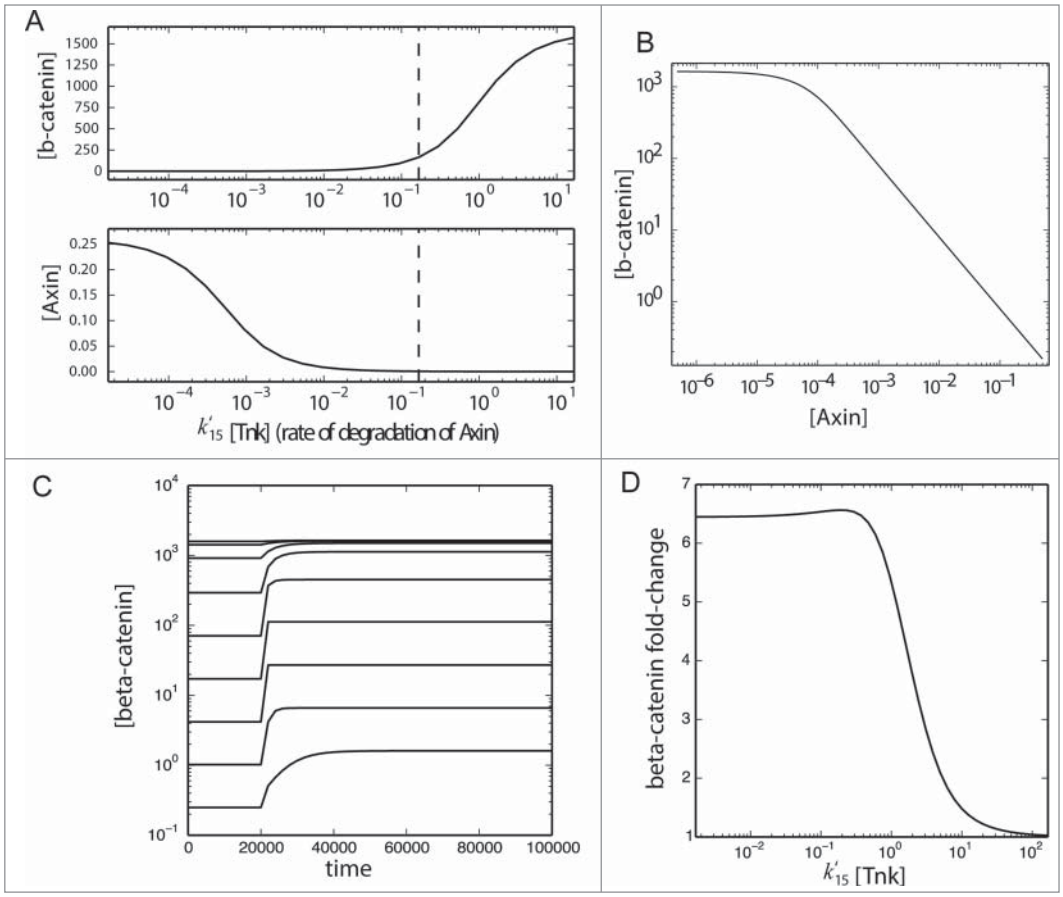

Figure 8. A model for bcat activity reveals differential responses to Tnk activity. The model of Lee et al.[52] and Goentoro and Kirschner[53] was modified such that Axin degradation (reaction 15) became linearly dependent on the concentration of Tankyrase [Tnk] with a new second-order kinetic constant k_{15}'. The value of k_{15}' was assumed to be equal to the value of k_{15} (0.167), and the basal concentration of Tankyrase was assumed to be 1 (in arbitrary units). Steady-state values of Axin and b-catenin concentration (brackets) were obtained from the simulation of the model under varying concentrations of Tankyrase (both above and below the basal concentration indicated by a dashed vertical line) and plotted as functions of the total rate of degradation of Axin (**A**) and as a parametric plot (**B**). Next, the model was run under different rates of Axin degradation (k15′[Tnk]) until it reached a steady state (s_1), then stimulated with addition of Wnt protein at t=20000 and run until a steady-state was again reached (s_2). These time courses were plotted to confirm a steady state was reached (**C**). For each value of k_{15}'[Tnk] the fold change in the steady-state of [β-catenin] was calculated (s1/s2) and plotted (**D**).

GSK-3 regulation of MTN positioning is independent of bcat activity

Our results reveal that BIO inhibits GSK-3 activity, leading to elevated bcat activity and an increase in the number of MTN neurons that show a more posterior location in the midbrain. In contrast, inhibition of bcat activity, through inhibition of Tankyrase enzyme or overexpression of dkk1, does not result in posteriorly located MTN neurons, but does lead to the formation of more neurons. As GSK-3 is important for regulating multiple intracellular signaling pathways, it may therefore have a bcat-independent role in controlling neurogenesis. To test if Wnt signaling can affect MTN positioning independently of GSK-3 function, we examined whether MTN development was altered in an *axin1* mutant, *masterblind* (*mbl*). We observe elevated *axin2* expression in *mbl* mutants indicative of increased bcat activity, similar to that observed after BIO treatment (**Fig. 9A and B**). We also note that *mbl* mutants have significantly more MTN neurons than in wildtype siblings, again similar to embryos treated with BIO (**Fig. 9C**). However, *mbl* mutants do not show posteriorly located neurons and there is no correlation between MTN number and positioning relative to the isthmus (**Fig. 9D and E**). This reveals that the increased number of MTN neurons caused by BIO treatment can be attributed to elevated bcat activity, but the posteriorly located MTN neurons observed in these embryos cannot be explained by increased bcat activity in the midbrain.

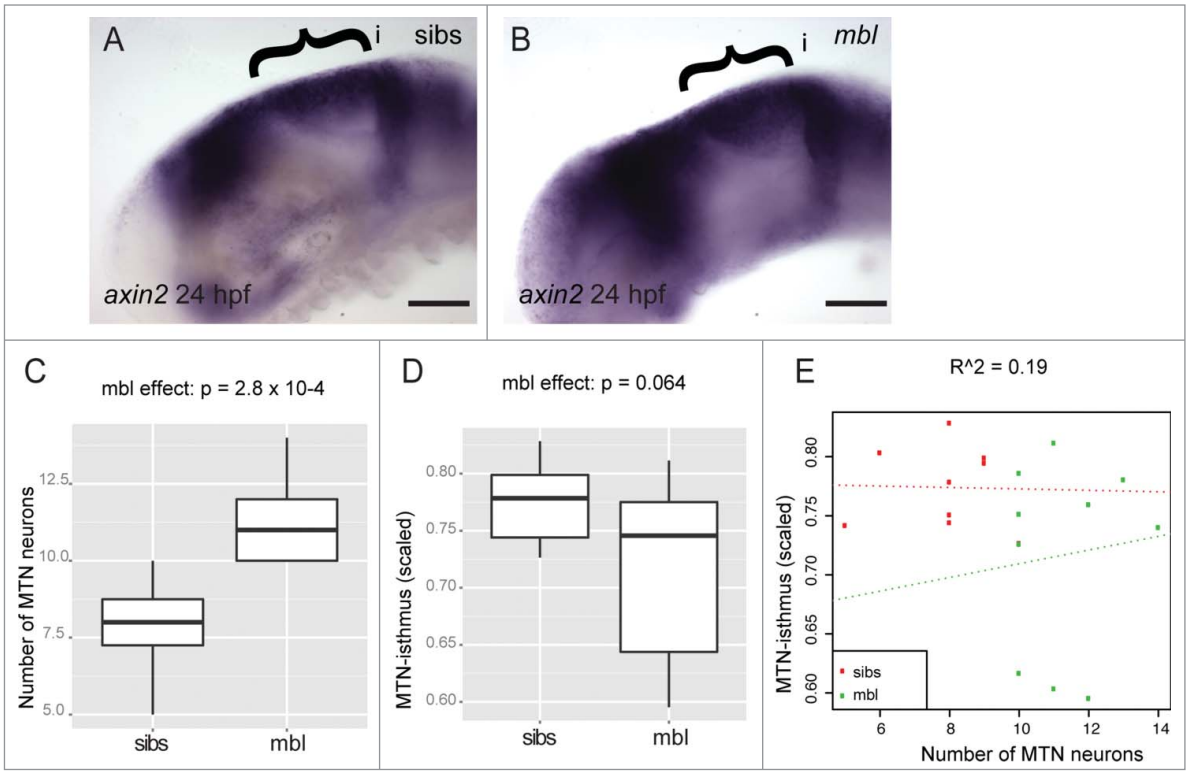

Figure 9. Masterblind mutants possess more MTN neurons, but do not show a posterior displacement of MTN neurons. Lateral views of 24 hpf embryos processed by *in situ* hybridization to reveal elevated *axin2* expression in midbrain (bracket) of *masterblind* mutants (*mbl*, **B**), relative to wildtype siblings (sibs, **A**). Box plot of the number of MTN neurons (**C**) or MTN-isthmus distance (scaled by midbrain size, **D**) in 24 hpf *mbl* mutants and sibs (n = 10 for each condition). There is a strong effect by *mbl* on MTN number ($p = 2.8 \times 10^{-4}$) but not on MTN-isthmus distance (p = 0.064). Dot plot of MTN number against MTN-isthmus distance (scaled) for *mbl* mutants and sibs (**E**). A line of best fit reveals no correlation between MTN neuron number and distance (R = 0.19, n = 10 for each condition). Isthmus (i). Scale bars: 100μM (**A,B**).

Discussion

We have addressed how the interplay between Wnt and FGF activity controls the spatiotemporal specification of neurons in the developing midbrain. Our findings reveal that a variety of feedback and feed-forward regulatory loops operate to control both the level and site of activity of each pathway. This has implications for where neurons form in the brain during development, but also how many neurons will form and thus affect progenitor cell populations important for later-forming neurons. We find that FGF activity controls the number and positioning of MTN neurons, whereas Wnt signaling is primarily important for controlling the number of neurons that form. Furthermore, we identify a putative role for GSK-3 in modulating FGF-target gene activity and hence neuronal positioning, independent of bcat function.

Previously we could show that FGF activity regulates the number and positioning of MTN neurons in the midbrain and that this is mediated by FGF control of *her5* expression. From these findings we predicted that alterations to FGF at early stages would affect subsequent development of later neuronal populations in the midbrain. We now present evidence that this occurs, as expansion of the MTN, due to reductions to FGF activity over a defined window of time, results in a smaller optic tectum. This reveals that a disruption to FGF activity across the midbrain upsets the controlled temporal onset of differentiation, needed for the appropriate spatial formation of discrete neuronal populations. Sustaining an appropriate level of FGF activity at the isthmus is therefore crucial for controlling where and when neurons are specified in the forming midbrain. There is a large body of evidence for an auto-regulatory interaction between Wnt and FGF signaling at the isthmus during midbrain development. Perturbations to this interaction are expected to affect midbrain patterning and development. In this study we have asked whether the interaction between Wnt and FGF occurs by control of bcat activity or of GSK-3. Inhibition of axin1 function, over-expression of dkk1 or over-activation of Axin function using IWR-1 all fail to alter MTN positioning, although they do increase the number of neurons that form. In contrast, GSK-3 inhibition promotes both the formation of extra neurons and the presence of posteriorly located neurons in the midbrain (**Fig. 10A**). We interpret these results to suggest that GSK-3 regulates FGF signaling across the midbrain independently of bcat. It further reveals that bcat activity controls the number of MTN neurons that form, independently of FGF signaling, but dependent on GSK-3 activity (**Fig. 10B**). Support for this interpretation comes from a screen to identify Wnt and FGF responsive genes in the developing tail bud of zebrafish.[56] Similar to our approach, LiCl

and SU5402 were used as tools to manipulate each pathway. Many genes examined showed similar responses to both GSK-3 inhibition and inhibition of FGF receptor function. Furthermore, it was shown that inhibition of GSK-3 by LiCl led to phosphorylation of ERK and therefore activation of ERK signaling. This was interpreted to suggest that Wnt/ bcat signaling was controlling FGF signaling through MAPK/ ERK activity. Based on our comparisons between BIO treatment relative to bcat overexpression, we would argue that GSK-3 has a bcat independent function in controlling MAPK/ERK activity.

We found that manipulations of bcat activity altered the number of MTN neurons that formed in the midbrain. This could be due to a role of Wnt signaling in controlling cell proliferation. Alternatively, it may reflect a role of Wnts in controlling neurogenesis. Recent findings have shown that Wnt/ bcat signaling can regulate neurogenesis in the flatworm *Platynereis* and regulates expression of neurogenic genes *Neurogenin1, Neurogenin2* and *NeuroD* in mouse.[24,25,57] We have previously shown that MTN development in the midbrain is not regulated by neurogenin function in zebrafish suggesting that Wnt/ bcat are not directing neuronal differentiation through regulation of *neurogenin* genes.[58] Intriguingly, the action of Wnt on neurogenesis in neural stem cells is influenced by the level of FGF activity.[33] We note that in zebrafish, increasing bcat activity promotes the formation of more MTN neurons. When this is performed in the context of reduced FGF activity (by varying doses of SU5402) this effect is enhanced. This implies that in the midbrain neuronal differentiation is controlled by the action of both FGF and Wnt/ bcat signaling. When this is perturbed by enhancing or reducing bcat activity (by expressing dkk1), we observe commensurate changes to the number of neurons that form in the midbrain. We have previously shown that temporal application of BIO at stages when MTN neurons start to differentiate does not alter proliferation, but does cause an increase in MTN number.[34] We suggest that this reveals a role of Wnt/ bcat signaling in controlling the process of neuronal differentiation in the midbrain.

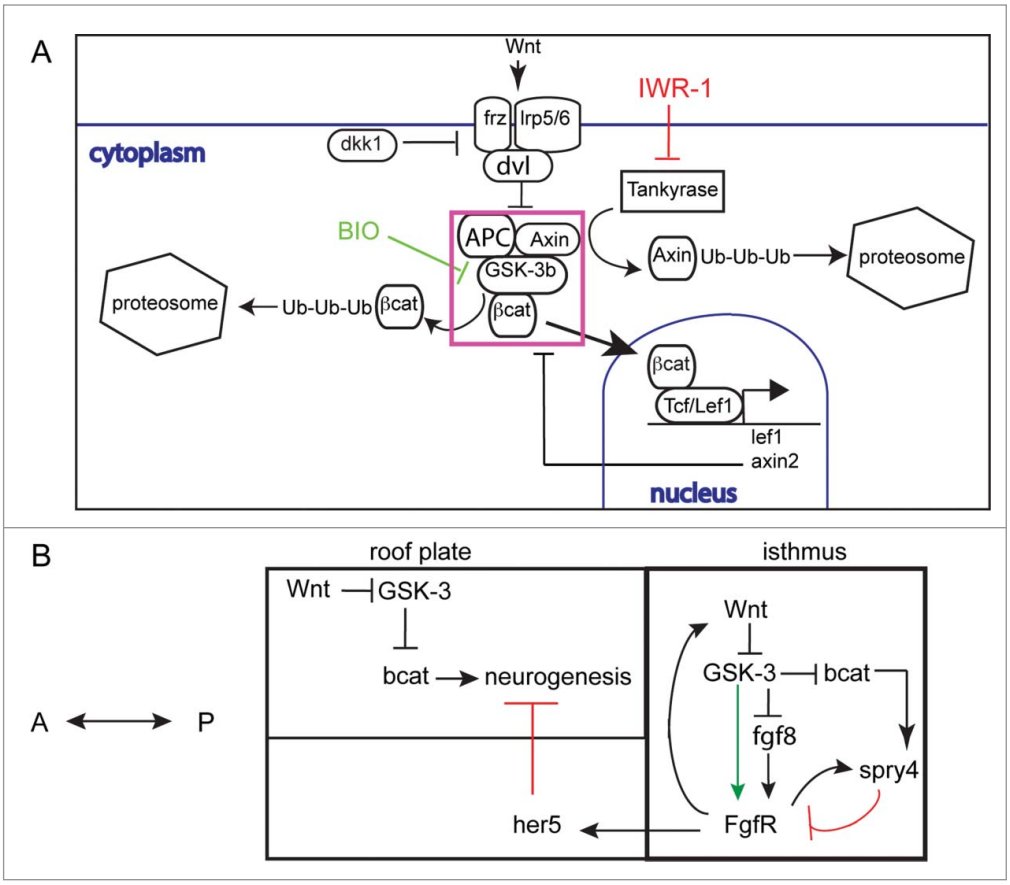

Figure 10. Schematic for interactions between Wnt/ bcat and FGF signaling during midbrain development (**A**). Secreted Wnt proteins bind frizzled (frz) and lrp5/6 cell membrane receptors complexed with dishevelled (dvl). This results in the inhibition of the ubiquitination (Ub) and subsequent degradation of bcat by the destruction complex (DC, purple box), incorporating Axin, APC and GSK-3 proteins. Free bcat concentration then rises and bcat can translocate to the nucleus to activate gene expression by binding TCF or LEF transcription factors. Inhibition of GSK-3 by BIO results in decreased bcat protein degradation. In contrast, inhibition of Tankyrase enzyme by IWR-1 prevents ubiquitination of Axin proteins and hence increased activity of the DC. A working model for Wnt-FGF interactions at the isthmus and in the midbrain during stages when MTN neurons form (**B**). Wnt and FGF signaling co-regulate each others activity in GSK-3 dependent and independent manners. Wnt inhibits GSK-3 activity leading to elevated bcat activity. *Spry4* expression is increased in response to bcat and FGF activity (FgfR) and acts to inhibit FgfR receptors. GSK-3 is also required for FgfR activity and acts independently of bcat activity (green arrow). FGF signaling across the midbrain represses neurogenesis through activation of her5; as the *her5* expression retracts posteriorly Wnt signaling acts to promote neuronal differentiation.

The targeted inhibition of Wnt/ bcat activity is important for treatment of many diseases and syndromes that involve aberrant Wnt signaling.[59] Tankyrase enzymes have been the focus for many such efforts, due to their important functions in degrading and so limiting Axin protein availability. The IWR and XAV939 compounds selectively inhibit Tnk, resulting in an increase in Axin protein and hence increased bcat degradation by the bcatDC.[11,53] Initial reports describing the effect of IWR-1 dose on bcat activity using the SuperTopFlash assay showed that an approximate linear response occurs relative to dose. We find that *in vivo*, IWR-1 does not affect bcat activity in a linear manner. We note that Wnt/ bcat responsive genes *lef1* and *spry4* show a

non-linear response to IWR-1 that changes relative to the duration of exposure. We also find that the concentration of IWR-1 alters the response over time. One intriguing observation we made is that low doses of IWR-1 initially cause a more severe inhibition of bcat responsive genes than a higher dose. Over time, higher concentrations of IWR-1 result in greater inhibition of bcat-dependent responses than lower concentrations. This change in response of bcat-responsive genes to different doses of IWR-1 suggests compensatory feedback loops modulate their response.

We have found that in the midbrain, FGF activity is required for expression of *wnt1* and controls bcat activity. Likewise, bcat is able to upregulate expression of *fgf8* and FGF target gene expression in the presence of SU5402. The interaction between Wnt and FGF signaling to maintain expression of their respective ligands in the isthmus is well established and occurs by a positive feedback loop.[3,4] One putative explanation for the differential effects of IWR-1 dosage on Wnt-target genes may therefore be due to feedback from FGF signaling to promote elevated bcat signaling. In support of this, we note that higher doses of IWR-1 causes a rapid decrease in bcat activity and leads to increased *wnt1* expression, similar to that seen by over-activation of FGF signaling. The varying response of bcat-dependent gene expression in relation to IWR-1 dose, suggests that FGF-dependent feedback loop induce an oscillatory response. Such oscillatory behavior is a prediction of models generated to explain robustness during Wnt/ bcat signaling.[50,60] Our interpretation of the results we observe *in vivo*, is that high doses of IWR-1 promote an FGF-mediated feedback mechanism leading to an upregulation of *wnt1* expression. Elevated levels of Wnt protein will promote bcatDC disassociation, until bcat-induced Axin2 levels rise sufficiently to overcome Wnt action on the bcatDC and bcat activity is then repressed. Our modification of a model for bcat activity indicates that when Axin degradation is low, the fold change is relatively insensitive to small changes in the degradation rate, but that it is far more sensitive to small changes at higher rates of degradation. This is result is analogous to previous analyses of bcat fold changes, which predicted sensitive and insensitive regions as a consequence of modifying the bcat degradation rate.[50] It would thus be valuable to further determine how the concentration of free bcat respond to differing concentrations of IWR-1 concentration over time and how this corresponds to the relative concentrations of Axin1 and Axin2. Even more importantly, it will be necessary to show how bcat-activated genes respond to Tnk inhibitors *in vivo*, to understand how robustness in signaling pathway activity impacts on the biological outputs of drugs that aim to modulate Wnt/ bcat.

In summary, we show that components of the Wnt/ bcat pathway controls 2 aspects of midbrain development. GSK-3 acts to modulate FGF activity at the isthmus and thus controls the spatiotemporal differentiation of early neuronal populations, such as the MTN, across the midbrain. This function of GSK-3 appears to be independent to its role in regulating bcat, which acts to control the number of neurons that form. How these 2 functions of Wnt signaling are integrated is unclear. One hypothesis is that GSK-3 is required for normal activation of intracellular FGF targets, such as ERK. Thus, the interplay between Wnt/ bcat and FGF signaling occurs at a number of levels and involves a complex set of feedback loops to control their relative activity. Perturbations to any one component will lead to compensatory activity, inducing some degree of oscillatory response. In the presence of small molecular inhibitors, which do not respond dynamically to such feedback loops, oscillations will be more pronounced until they eventually reach a new equilibrium. As recently highlighted, this is relevant for understanding how cells *in vivo* may respond to drugs that target Wnt/ bcat activity.[59] It is therefore crucial to target the most appropriate component of this pathway for effective inhibition of bcat activity with minimal interference to other important signaling pathways.

Disclosure of Potential Conflicts of Interest

No potential conflicts of interest were disclosed.

Acknowledgments

We would like to thank Lea Goentoro and Marc Kirschner for sharing their models for Wnt/ bcat signaling. Also, Karen Liu, Joao Peres, Holger Bielen, Corinne Houart, Geraint Thomas for constructive discussions and reagents.

References

1. Barkovich AJ, Millen KJ, Dobyns WB. A developmental and genetic classification for midbrain-hindbrain malformations. Brain 2009; 132:3199-230; PMID:19933510; http://dx.doi.org/10.1093/brain/awp247
2. Raible F, Brand M. Divide et Impera–the midbrain-hindbrain boundary and its organizer. Trends Neurosci 2004; 27:727-34; PMID:15541513
3. Wurst W, Bally-Cuif L. Neural plate patterning: upstream and downstream of the isthmic organizer. Nat Rev Neurosci 2001; 2:99-108; PMID:11253000
4. Rhinn M, Brand M. The midbrain–hindbrain boundary organizer. Curr Opin Neurobiol 2001; 11:34-42; PMID:11179870
5. Crossley PH, Martinez S, Martin GR. Midbrain development induced by FGF8 in the chick embryo. Nature 1996; 380:66-8; PMID:8598907
6. Martinez S, Crossley PH, Cobos I, Rubenstein JL, Martin GR. FGF8 induces formation of an ectopic isthmic organizer and isthmocerebellar development via a repressive effect on Otx2 expression. Development 1999; 126:1189-200; PMID:10021338
7. Reifers F, Bohli H, Walsh EC, Crossley PH, Stainier DY, Brand M. Fgf8 is mutated in zebrafish acerebellar (ace) mutants and is required for maintenance of midbrain-hindbrain boundary development and somitogenesis. Development 1998; 125:2381-95; PMID:9609821
8. Geling A, Itoh M, Tallafuss A, Chapouton P, Tannhauser B, Kuwada JY, Chitnis AB, Bally-Cuif L. bHLH transcription factor Her5 links patterning to regional inhibition of neurogenesis at the midbrain-hindbrain boundary. Development 2003; 130:1591-604; PMID:12620984
9. Scholpp S, Lohs C, Brand M. Engrailed and Fgf8 act synergistically to maintain the boundary between diencephalon and mesencephalon. Development 2003; 130:4881-93; PMID:12917294
10. Partanen J. FGF signalling pathways in development of the midbrain and anterior hindbrain. J Neurochem 2007; 101:1185-93; PMID:17326764
11. Huang SM, Mishina YM, Liu S, Cheung A, Stegmeier F, Michaud GA, Charlat O, Wiellette E, Zhang Y, Wiessner S, et al. Tankyrase inhibition stabilizes axin and antagonizes Wnt signalling. Nature 2009; 461:614-20; PMID:19759537; http://dx.doi.org/10.1038/nature08356
12. Lahti L, Saarimaki-Vire J, Rita H, Partanen J. FGF signaling gradient maintains symmetrical proliferative divisions of midbrain neuronal progenitors. Dev Biol 2011; 349:270-82; PMID:21074523; http://dx.doi.org/10.1016/j.ydbio.2010.11.008
13. Ye W, Shimamura K, Rubenstein JL, Hynes MA, Rosenthal A. FGF and Shh signals control dopaminergic and serotonergic cell fate in the anterior neural plate. Cell 1998; 93:755-66; PMID:9630220
14. Jaeger I, Arber C, Risner-Janiczek JR, Kuechler J, Pritzsche D, Chen IC, Naveenan T, Ungless MA, Li M. Temporally controlled modulation of FGF/ERK signaling directs midbrain dopaminergic neural progenitor fate in mouse and human pluripotent stem cells.

Development 2011; 138:4363-74; PMID:21880784; http://dx.doi.org/10.1242/dev.066746
15. Bosco A, Bureau C, Affaticati P, Gaspar P, Bally-Cuif L, Lillesaar C. Development of hypothalamic serotoninergic neurons requires Fgf signalling via the ETS-domain transcription factor Etv5b. Development 2013; 140:372-84; PMID:23250211; http://dx.doi.org/10.1242/dev.089094
16. Jaszai J, Reifers F, Picker A, Langenberg T, Brand M. Isthmus-to-midbrain transformation in the absence of midbrain-hindbrain organizer activity. Development 2003; 130:6611-23; PMID:14660549
17. Basson MA, Echevarria D, Ahn CP, Sudarov A, Joyner AL, Mason IJ, Martinez S, Martin GR. Specific regions within the embryonic midbrain and cerebellum require different levels of FGF signaling during development. Development 2008; 135:889-98; PMID:18216176; http://dx.doi.org/10.1242/dev.011569
18. Niehrs C, Acebron SP. Mitotic and mitogenic Wnt signalling. EMBO J 2012; 31:2705-13; PMID:22617425; http://dx.doi.org/10.1038/emboj.2012
19. Paridaen JT, Danesin C, Elas AT, van de Water S, Houart C, Zivkovic D. Apc1 is required for maintenance of local brain organizers and dorsal midbrain survival. Dev Biol 2009; 331:101-12; PMID:19397905; http://dx.doi.org/10.1016/j.ydbio.2009.04.022
20. McMahon AP, Joyner AL, Bradley A, McMahon JA. The midbrain-hindbrain phenotype of Wnt-1-/Wnt-1- mice results from stepwise deletion of engrailed-expressing cells by 9.5 days postcoitum. Cell 1992; 69:581-95; PMID:1534034
21. Thomas KR, Capecchi MR. Targeted disruption of the murine int-1 proto-oncogene resulting in severe abnormalities in midbrain and cerebellar development. Nature 1990; 346:847-50; PMID:2202907
22. Rhinn M, Picker A, Brand M. Global and local mechanisms of forebrain and midbrain patterning. Curr Opin Neurobiol 2006; 16:5-12; PMID:16418000
23. Mulligan KA, Cheyette BN. Wnt signaling in vertebrate neural development and function. J Neuroimmune Pharmacol 2012; 7:774-87; PMID:23015196; http://dx.doi.org/10.1007/s11481-012-9404-x
24. Hirabayashi Y, Itoh Y, Tabata H, Nakajima K, Akiyama T, Masuyama N, Gotoh Y. The Wnt/β-catenin pathway directs neuronal differentiation of cortical neural precursor cells. Development 2004; 131:2791-801; PMID:15142975
25. Qu Q, Sun G, Murai K, Ye P, Li W, Asuelime G, Cheung YT, Shi Y. Wnt7a regulates multiple steps of neurogenesis. Mol Cell Biol 2013; 33:2551-9; PMID:23629626; http://dx.doi.org/10.1128/MCB.00325-13
26. Yang J, Brown A, Ellisor D, Paul E, Hagan N, Zervas M. Dynamic temporal requirement of Wnt1 in midbrain dopamine neuron development. Development 2013; 140:1342-52; PMID:23444360; http://dx.doi.org/10.1242/dev.080630
27. Castelo-Branco G, Rawal N, Arenas E. GSK-3beta inhibition/β-catenin stabilization in ventral midbrain precursors increases differentiation into dopamine neurons. J Cell Sci 2004; 117:5731-7; PMID:15522889
28. Joksimovic M, Yun BA, Kittappa R, Anderegg AM, Chang WW, Taketo MM, McKay RD, Awatramani RB. Wnt antagonism of Shh facilitates midbrain floor plate neurogenesis. Nat Neurosci 2009; 12:125-31; PMID:19122665; http://dx.doi.org/10.1038/nn.2243
29. Tang M, Miyamoto Y, Huang EJ. Multiple roles of β-catenin in controlling the neurogenic niche for midbrain dopamine neurons. Development 2009; 136:2027-38; PMID:19439492; http://dx.doi.org/10.1242/dev.034330
30. Alves dos Santos MT, Smidt MP. En1 and Wnt signaling in midbrain dopaminergic neuronal development. Neural Dev 2011; 6:23; PMID:21569278; http://dx.doi.org/10.1186/1749-8104-6-23
31. Canning CA, Lee L, Irving C, Mason I, Jones CM. Sustained interactive Wnt and FGF signaling is required to maintain isthmic identity. Dev Biol 2007; 305:276-86; PMID:17383629
32. Wittmann DM, Blochl F, Trumbach D, Wurst W, Prakash N, Theis FJ. Spatial analysis of expression patterns predicts genetic interactions at the mid-hindbrain boundary. PLoS Comput Biol 2009; 5:e1000569; PMID:19936059; http://dx.doi.org/10.1371/journal.pcbi.1000569
33. Israsena N, Hu M, Fu W, Kan L, Kessler JA. The presence of FGF2 signaling determines whether β-catenin exerts effects on proliferation or neuronal differentiation of neural stem cells. Dev Biol 2004; 268:220-31; PMID:15031118
34. Dyer C, Blanc E, Hanisch A, Roehl H, Otto GW, Yu T, Basson MA, Knight R. A bi-modal function of Wnt signalling directs an FGF activity gradient to spatially regulate neuronal differentiation in the midbrain. Development 2014; 141:63-72; PMID:24284206; http://dx.doi.org/10.1242/dev.099507
35. Geling A, Plessy C, Rastegar S, Strahle U, Bally-Cuif L. Her5 acts as a prepattern factor that blocks neurogenin1 and coe2 expression upstream of Notch to inhibit neurogenesis at the midbrain-hindbrain boundary. Development 2004; 131:1993-2006; PMID:15056616
36. Ninkovic J, Tallafuss A, Leucht C, Topczewski J, Tannhauser B, Solnica-Krezel L, Bally-Cuif L. Inhibition of neurogenesis at the zebrafish midbrain-hindbrain boundary by the combined and dose-dependent activity of a new hairy/E(spl) gene pair. Development 2005; 132:75-88; PMID:15590746
37. Tallafuss A, Bally-Cuif L. Tracing of her5 progeny in zebrafish transgenics reveals the dynamics of midbrain-hindbrain neurogenesis and maintenance. Development 2003; 130:4307-23; PMID:12900448
38. Westerfield M. The zebrafish book: A guide for laboratory use of the zebrafish *Danio rerio*. Eugene, Oregon: University of Oregon Press; 2007.
39. Heisenberg CP, Houart C, Take-Uchi M, Rauch GJ, Young N, Coutinho P, Masai I, Caneparo L, Concha ML, Geisler R, et al. A mutation in the Gsk3-binding domain of zebrafish Masterblind/Axin1 leads to a fate transformation of telencephalon and eyes to diencephalon. Genes Dev 2001; 15:1427-34; PMID:11390362
40. Park HC, Kim CH, Bae YK, Yeo SY, Kim SH, Hong SK, Shin J, Yoo KW, Hibi M, Hirano T, et al. Analysis of upstream elements in the HuC promoter leads to the establishment of transgenic zebrafish with fluorescent neurons. Dev Biol 2000; 227:279-93; PMID:11071755
41. Molina GA, Watkins SC, Tsang M. Generation of FGF reporter transgenic zebrafish and their utility in chemical screens. BMC Dev Biol 2007; 7:62; PMID:17553162
42. Weidinger G, Thorpe CJ, Wuennenberg-Stapleton K, Ngai J, Moon RT. The Sp1-related transcription factors sp5 and sp5-like act downstream of Wnt/β-catenin signaling in mesoderm and neuroectoderm patterning. Curr Biol 2005; 15:489-500; PMID:15797017
43. Gonzalez-Quevedo R, Lee Y, Poss KD, Wilkinson DG. Neuronal regulation of the spatial patterning of neurogenesis. Dev Cell 2010; 18:136-47; PMID:20152184; http://dx.doi.org/10.1016/j.devcel.2009.11.010
44. Scheer N, Campos-Ortega JA. Use of the Gal4-UAS technique for targeted gene expression in the zebrafish. Mech Dev 1999; 80:153-8; PMID:10072782
45. Zerucha T, Stuhmer T, Hatch G, Park BK, Long Q, Yu G, Gambarotta A, Schultz JR, Rubenstein JL, Ekker M. A highly conserved enhancer in the Dlx5/Dlx6 intergenic region is the site of cross-regulatory interactions between Dlx genes in the embryonic forebrain. J Neurosci 2000; 20:709-21; PMID:10632600
46. Dorsky RI, Sheldahl LC, Moon RT. A transgenic Lef1/β-catenin-dependent reporter is expressed in spatially restricted domains throughout zebrafish development. Dev Biol 2002; 241:229-37; PMID:11784107
47. Thisse B, Thisse C. Fast Release Clones: A High Throughput Expression Analysis. ZFIN Direct Data Submission 2004; ZFIN ID: ZDB-PUB-040907-1
48. Nusslein-Volhard C, Dahm R. Zebrafish: A Practical Approach (The Practical Approach Series, 261). Oxford, England: Oxford University Press; 2002.
49. Lee E, Salic A, Kruger R, Heinrich R, Kirschner MW. The roles of APC and Axin derived from experimental and theoretical analysis of the Wnt pathway. PLoS Biol 2003; 1:E10; PMID:14551908
50. Goentoro L, Kirschner MW. Evidence that fold-change, and not absolute level, of β-catenin dictates Wnt signaling. Mol Cell 2009; 36:872-84; PMID:20005849; http://dx.doi.org/10.1016/j.molcel.2009.11.017
51. Hjorth JT, Key B. Are pioneer axons guided by regulatory gene expression domains in the zebrafish forebrain? High-resolution analysis of the patterning of the zebrafish brain during axon tract formation. Dev Biol 2001; 229:271-86; PMID:11203695
52. Moro E, Ozhan-Kizil G, Mongera A, Beis D, Wierzbicki C, Young RM, Bournele D, Domenichini A, Valdivia LE, Lum L, et al. In vivo Wnt signaling tracing through a transgenic biosensor fish reveals novel activity domains. Dev Biol 2012; 366:327-40; PMID:22546689; http://dx.doi.org/10.1016/j.ydbio.2012.03.023
53. Chen B, Dodge ME, Tang W, Lu J, Ma Z, Fan CW, Wei S, Hao W, Kilgore J, Williams NS, et al. Small molecule-mediated disruption of Wnt-dependent signaling in tissue regeneration and cancer. Nat Chem Biol 2009; 5:100-7
54. Kofahl B, Wolf J. Mathematical modelling of Wnt/β-catenin signalling. Biochem Soc Trans 2010; 38:1281-5; PMID:20863299; http://dx.doi.org/10.1042/BST0381281
55. Goentoro L, Shoval O, Kirschner MW, Alon U. The incoherent feedforward loop can provide fold-change detection in gene regulation. Molecular cell 2009; 36:894-9.; PMID:20005851; http://dx.doi.org/10.1016/j.molcel.2009
56. Stulberg MJ, Lin A, Zhao H, Holley SA. Crosstalk between Fgf and Wnt signaling in the zebrafish tailbud. Dev Biol 2012; 369:298-307; PMID:22796649; http://dx.doi.org/10.1016/j.ydbio.2012.07.003
57. Demilly A, Steinmetz P, Gazave E, Marchand L, Vervoort M. Involvement of the Wnt/β-catenin pathway in neurectoderm architecture in Platynereis dumerilii. Nat Commun 2013; 4:1915; PMID:23715274; http://dx.doi.org/10.1038/ncomms2915
58. Dyer C, Linker C, Graham A, Knight R. Specification of sensory neurons occurs through diverse developmental programs functioning in the brain and spinal cord. Dev Dyn 2014; 243:1429-39; PMID:25179866; http://dx.doi.org/10.1002/dvdy.24184
59. Kahn M. Can we safely target the WNT pathway? Nat Rev Drug Discov 2014; 13:513-32; PMID:24981364; http://dx.doi.org/10.1038/nrd4233
60. Wawra C, Kuhl M, Kestler HA. Extended analyses of the Wnt/β-catenin pathway: robustness and oscillatory behaviour. FEBS Lett 2007; 581:4043-8; PMID:17678900